National Conference with International Participation

ENGINEERING MECHANICS 2008

Svratka, Czech Republic, May 12 – 15, 2008

STUDY OF ADAPTIVE CONTROL ALGORITHM EMPLOYING HYSTERETIC MAGNETO-RHEOLOGICAL DAMPER MODEL IN ¼ CAR SUSPENSION

J. Úradníček*, M. Musil**

Summary: *This paper presents a study of the semiactive adaptive control algorithm through numerical simulation where the adaptive control is compared to the skyhook control, active LQR, semiactive LQR and passive suspension. A hysteretic magneto-rheological (MR) damper model is proposed so that sensitivity of the system variables with respect to the control variable can be evaluated for the purpose of employing the adaptive control algorithm based on the gradient search method. This study includes discussions of the MR damper model setup ¼-car suspension model setup, controller setup and dynamic analysis approach. The effectiveness of all controllers and passive suspension is demonstrated through simulations.*

1. Introduction

Since Semiactive control policy was first developed by Karnopp and Crosby in the 1973, great attention has been paid to the development of a semiactive suspension for automotive applications, which introduced many improvements of the original Skyhook strategy proposed in (Crosby et al., 1973).

Non-model based Skyhook control is a bi-state control policy which is along its variations widely used in a seats suspension or car suspension assembly. The amount of dissipated energy in a semiactive damper is controlled through the changing of damper characteristics. Even though the skyhook is a relatively simple and low-cost policy verified by many years of usage, there are some circumstances when skyhook could yield adverse results. One of the main disadvantages of the skyhook policy is the result of higher harmonics occurring in a system which should nevertheless have pure tone signals accessing it. This higher harmonic is the cause of nonlinearity due to switching between two states of controlled semiactive damper. Another disadvantage is the dynamical jerking occurring due to phase delay as a result of the application of filters to derive relative velocity from the measured displacement signal. These dynamical phenomena are explained in (Ahmedian et al., 2001). The third non-

* Ing. Juraj Úradníček.: Institute of applied mechanics and mechatronics, Slovak University of Technology in Bratislava, Nam. slobody 17, 812 31 Bratislava 1;
tel.: +421 212 572 96 404, fax: +421 212 5249 7890; e-mail: juraj.uradnicek@stuba.sk

** Doc. Ing. Milos Musil, PhD.: Institute of applied mechanics and mechatronics, Slovak University of Technology in Bratislava, Nam. slobody 17, 812 31 Bratislava 1;
tel.: +421 212 572 96 389, fax: +421 212 5249 7890; e-mail: milos.musil@stuba.sk

negligible weakness of the skyhook is its poor adaptability to plant variations or different excitation profiles. Skyhook gain is pre-tuned in certain conditions according to a performance index. Changing this conditions can leads to worse or even adverse performance.

Mentioned disadvantages of the skyhook strategy can be attenuated introducing an adaptive control strategy which can control damper characteristics continuously (Song et al., 2004). Since the performance index is evaluated in real time, such a strategy can react to the plant and road variations immediately.

Reasonable MR damper model should be employed in order to use the model-based adaptive control algorithm which requires the calculation of the sensitivity of controlled variables with respect to the control current applied to the MR damper. Modeling of the MR damper is discussed in (Hong et al., 2005).

2. Modeling of semiactive MR damper

In order to use the model-based adaptive control algorithm a simple hysteretic semiactive MR damper model has been proposed to ensure easy differentiability of a whole system model with respect to the control current *I*. Force F_{MR} produced in the MR damper is calculated from

$$F_{MR} = m_f^* \ddot{x}_r + c_f \dot{x}_r + F_y \tanh(\beta \dot{x}_r) \quad (1)$$

$$m_f^* \ddot{x}_r + c_f \dot{x}_r + F_y \tanh(\beta \dot{x}_r) + k_1 x_r = k_1 \emptyset x_1, \quad (2)$$

where m_f^* - mass effect of MR fluid, c_f - viscous damping effect of the flow resistance in the electrode in the absence of the magnetic field, F_y - yield force which can be controlled by the magnetic field, $\emptyset = k_2/k_1$, $k_{1,2}$ - spring effect of MR damper representing the compliance effect of chambers, x_r – evolutionary variable which represent relative displacement of fluid inertance, β - geometrical constant, x_1 – relative displacement of the damper piston. All mentioned parameters are subject to identification.

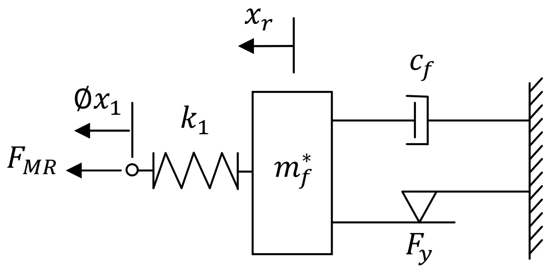

Fig. 1: mechanical model of MR damper

Friction force due to polarized MR fluid passing through the electrode gap in MR damper is often modeled as Coulomb friction using 'sign(·)' function. However, it can cause problems in simulation due to properties of 'sign(·)' function. Moreover, adaptive algorithm proposed in this paper requires continuous mathematical model which can be differentiated with respect to the electric current applied to the MR damper. Under this consideration friction force in (1), (2) is modeled by the 'tanh(·)' function where parameter β describes how rapidly friction force changes when MR fluid inertance velocity $\dot{x}_r$ comes from negative to positive values and vice-versa.

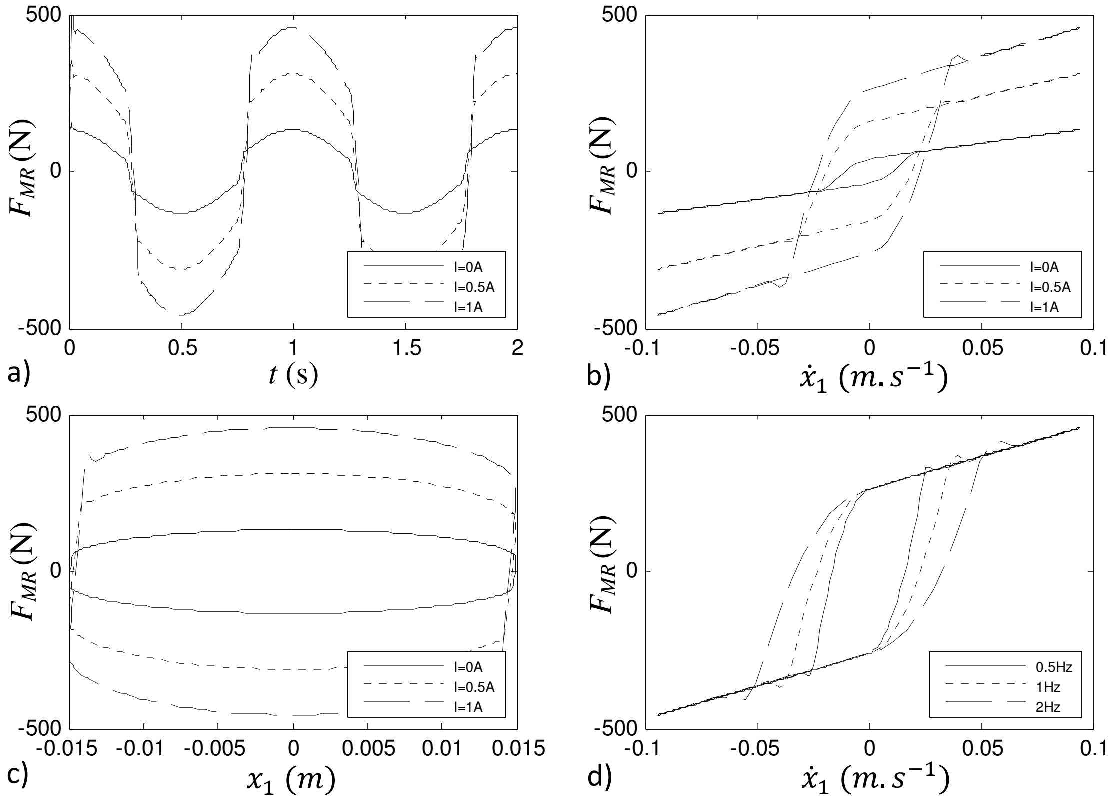

Fig. 2: calculated damping force vs. a) time, b) piston velocity, c) piston displacement for excitation frequency 1Hz and various current *I*, d) damping force vs. piston velocity for the same current *I*=1A and various excitation frequency.

3. Suspension system description

The same mathematical model is considered for the both active Fig.3.a and semiactive Fig.3.b suspension, but in the semiactive case active force *u* is replaced by semiactive force produced due to energy dissipation in MR damper and spring energy storage, which stiffness can be represented by nonlinear function in general.

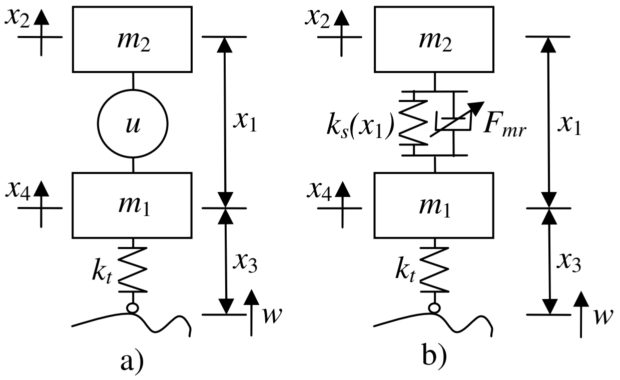

Fig. 3: mechanical model of a) active, b) semiactive quarter car suspension

System dynamics can be represented in state space as follows

$$\dot{\boldsymbol{x}}(t) = \boldsymbol{A}\boldsymbol{x}(t) + \boldsymbol{B}u(t) + \boldsymbol{L}\dot{w}(t) \tag{3}$$

$$\boldsymbol{y}(t) = \boldsymbol{C}\boldsymbol{x}(t) + \boldsymbol{D}u(t), \tag{4}$$

where $\boldsymbol{x} = [x_1,\ \dot{x}_2,\ x_3,\ \dot{x}_4]$T is the state vector, $\boldsymbol{y} = [\ddot{x}_2,\ x_1,\ x_3]$T is the output vector, w represents a road excitation and matrices A, B, C, D, L have the following structure

$$\boldsymbol{A} = \begin{bmatrix} 0 & 1 & 0 & -1 \\ 0 & 0 & 0 & 0 \\ 0 & 0 & 0 & 1 \\ 0 & 0 & -\frac{k_t}{m_1} & 0 \end{bmatrix}, \boldsymbol{B} = \begin{bmatrix} 0 \\ -\frac{1}{m_2} \\ 0 \\ \frac{1}{m_1} \end{bmatrix}, \boldsymbol{C} = \begin{bmatrix} 0 & 0 & 0 & 0 \\ 1 & 0 & 0 & 0 \\ 0 & 0 & 1 & 0 \end{bmatrix}, \boldsymbol{D} = \begin{bmatrix} -\frac{1}{m_2} \\ 0 \\ 0 \end{bmatrix}, \boldsymbol{L} = \begin{bmatrix} 0 \\ 0 \\ -1 \\ 0 \end{bmatrix}.$$

The output vector $\boldsymbol{y}$ structure has been chosen in sense of formulation the performance index in next chapter.

4. Control strategy

Three different strategies to control active/semiactive suspension force are compared to each other. The firs approach to design an active law for suspension system is LQR control (Tewari, 2002)**,** such an idea has been initially proposed by (Thompson et al., 1976)**.** LQR control is also demonstrated on semiactive suspension setup, where active force is approximated by semiactive force or applied current to the MR damper is varied in such way to generate control force as close as possible to the target active force. This strategy is known as a 'clipped control', which could be done due to mathematical model of MR damper utilized to predict semiactive damper force F_{mr}.

The third approach is the skyhook control which is easy to implement to the real suspension, hence it is non-model based control strategy without need to predict semiactive force or actual system state. Semiactive force is controlled directly just upon the measured data following skyhook rule.

The last control strategy is gradient-based adaptive algorithm (Song et al., 2004) which requires differentiable mathematical description of the controlled mechanical system including MR damper by reason of derive the performance index sensitivity with respect to the controlled damper current.

4.1. LQR active control

Firstly the state variables that are supposed to be minimized by the given control law are chosen. Concerned variables are the sprung mass acceleration $\ddot{x}_2$, the relative suspension displacement x_1 and the tire deformation x_3 all included in the output vector $\boldsymbol{y}$. Because of trade off between performance and comfort it is necessary to formulate performance index to ensure reasonable compromise. Performance index is given by the quadratic form

$$J(u) = \int_0^\infty (\ddot{x}_2^2 + q_1 x_1^2 + q_2 x_3^2 + r u^2) dt \tag{5}$$

in the matrix form

$$J(u) = \int_0^\infty (\boldsymbol{y}^T \boldsymbol{Q} \boldsymbol{y} + u^T r u) dt \tag{6}$$

where matrix $\boldsymbol{Q} = diag\{1, q_1, q_2\}$ is the matrix of weighting constants and r is the constant putting weight on the active force in order to minimize the suspension energy requirements. According to (Tewari, 2002) minimizing of the functional (6) can be done by the simple solution of the algebraic Riccati equation and the solution takes the form of a feedback control law

$$u(t) = -\boldsymbol{K} x(t). \tag{7}$$

4.2. LQR semiactive clipped control

Since the semiactive damper combined with the passive spring can't generate the active force, semiactive control law is rather limited against the fully active control. All it can do is to manage the dissipation and the storage of the energy (in case of pneumatic spring) in that way to follows the fully active force as close as possible. Accordingly, the current applied to the MR damper is controlled in that way to minimize the norm

$$P = |u(t) - u_s(t)|, \tag{8}$$

where semiactive control force

$$u_s(t) = k_s(x_1) x_1 + F_{MR}(\dot{x}_1, I). \tag{9}$$

The electric current which minimizes P can be denoted as I^* given by

$$I^* = \arg \min_{I \in +R^+} P(I) \tag{10}$$

In our simulation study the seven MR forces for seven electric currents (0A-6A) are computed using proposed MR damper model and I^* is chosen in each time step according to rule (10).

4.3. Skyhook control

Skyhook control policy in this study is represented by the following control rule

$$I = \begin{cases} 0 & \dot{x}_2 x_1 \leq 0 \\ S_{sky}\dot{x}_2 x_1 & \dot{x}_2 x_1 > 0 \end{cases} \tag{11}$$

It can be seen that just measurement of the sprung mass velocity and relative suspension displacement has to be known in case of skyhook control. Skyhook gain S_{sky} is subjected to the optimization according to driving conditions and requirements on suspension.

4.4. Adaptive control

Electric current *I* in the gradient-based algorithm is governed by the rule

$$I(t + \Delta\text{t}) = I(t) + \mu\left(-\frac{\partial J_a}{\partial I}\right) \tag{12}$$

$$J_a(t) = \ddot{x}_2^2(t) + q_1 x_1^2(t) + q_2 x_3^2(t). \tag{13}$$

By reason of nonlinear control algorithm, which always tries to minimize performance index (13) regardless of plant variations and on-going unknown excitations in each time step, the performance index isn`t the form of the integral criterion as (5) is. At the same time minimizing of the power requirements fitted in (5) isn't considered here. Constant μ is the adaptive algorithm gain and is determined so that the algorithm converges to the optimal control for given driving conditions.

Sensitivity of the performance index with respect to the control current $\frac{\partial J_a}{\partial I}$ can be found differentiating (13) with respect to *I*

$$\frac{\partial J_a}{\partial I} = 2\ddot{x}_2\frac{\partial \ddot{x}_2}{\partial I} + 2q_1 x_1\frac{\partial x_1}{\partial I} + 2q_2 x_3\frac{\partial x_3}{\partial I}. \tag{14}$$

Now, sensitivity of the state variables with respect to *I* are obtained differentiating equations (3), (4) with respect to *I*

$$\frac{\partial \dot{\boldsymbol{x}}}{\partial I} = \boldsymbol{A}\frac{\partial \boldsymbol{x}}{\partial I} + \boldsymbol{B}\frac{\partial u_s}{\partial I} \tag{15}$$

$$\frac{\partial \boldsymbol{y}}{\partial I} = \boldsymbol{C}\frac{\partial \boldsymbol{x}}{\partial I} + \boldsymbol{D}\frac{\partial u_s}{\partial I}. \tag{16}$$

It can be noticed that excitation $w(t)$ in (3) doesn't depend on applied current *I* such that there is no sensitivity. In semiactive force u_s (9) only the current dependent part is dissipative force generated in MR damper which can be obtained differentiating (1), (2) with respect to *I*

$$m_f^*\frac{\partial \ddot{x}_r}{\partial I} + \frac{\partial c_f x_r}{\partial I} + \frac{\partial F_y \tanh(\beta\dot{x}_r)}{\partial I} \tag{17}$$

$$m_f^*\frac{\partial \ddot{x}_r}{\partial I} + \frac{\partial c_f x_r}{\partial I} + \frac{\partial F_y \tanh(\beta\dot{x}_r)}{\partial I} + \frac{\partial k_1 x_r}{\partial I} = \frac{\partial k_1 \emptyset x_1}{\partial I} \tag{18}$$

5. Simulation

Simulations of the ¼ car model has been implemented in the program MATLAB®.

The first simulation presents system response to the sine sweep excitation Fig.4.a with decreasing amplitude passing through the system. Sweeping frequency ranges from 0.5 to 4 Hz. The first passive system resonant frequency is 1.1 Hz. The amplitude of signal linearly decreases with time from start (3cm) to finish (1cm). This excitation has been used to tune single control policies as well as to find optimal passive damping in the sense of minimizing performance index (5) over the 10 second time interval.

Second simulation presents system response to the random excitation Fig.4.b with PSD distribution function

$$S(\omega) = \frac{cV}{\omega^2 + \alpha^2 V^2}, \tag{19}$$

where $c = (\frac{\sigma^2}{\pi})\alpha$. Here σ^2denotes the road roughness variance and V the vehicle speed, whereas the coefficients c and α depend on the type of road surface. Values of the coefficients used in the simulations can be seen in Tab.1.

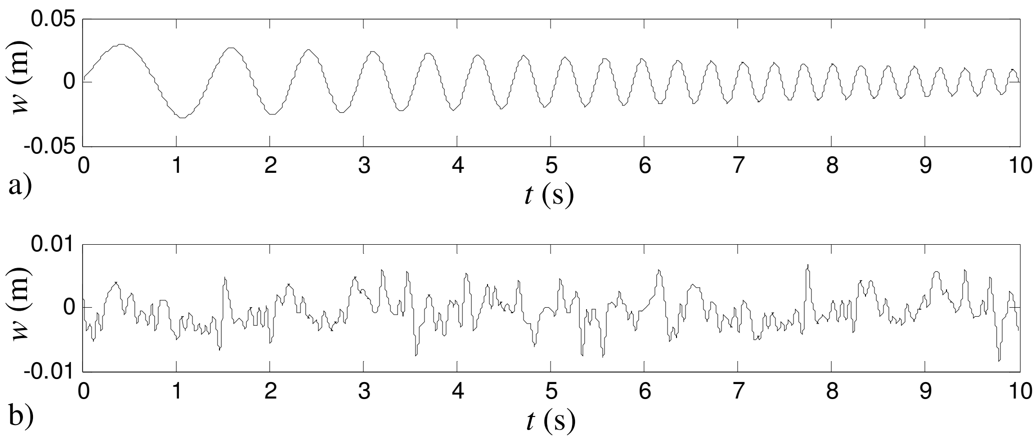

Fig. 4: System excitation a) sweep sine b) random road profile

Tab. 1: Coefficients used in the simulations

F_y =199.8+67.1 $I^{1.57}$	$m_f^* = 2.959$	c_f= 1055-70 I	k_1 = 326750-266625 I
k_2 = 1533000+194000 I	m_1=28.58 (kg)	m_2=288.9 (kg)	k_t = 155900 (kg/m)
k_s = 14000 (kg/m)	q_1 = 5e3	q_2 = 5e4	r = 0
K=[-20428, -3468, 2920, 861]	V = 30 (m/s)	σ^2 = 7 (mm^2)	α = 0.15 (m^{-1})
S_{sky} = 5e3	μ = 1e-4	β = 100	Δt = 1e-5

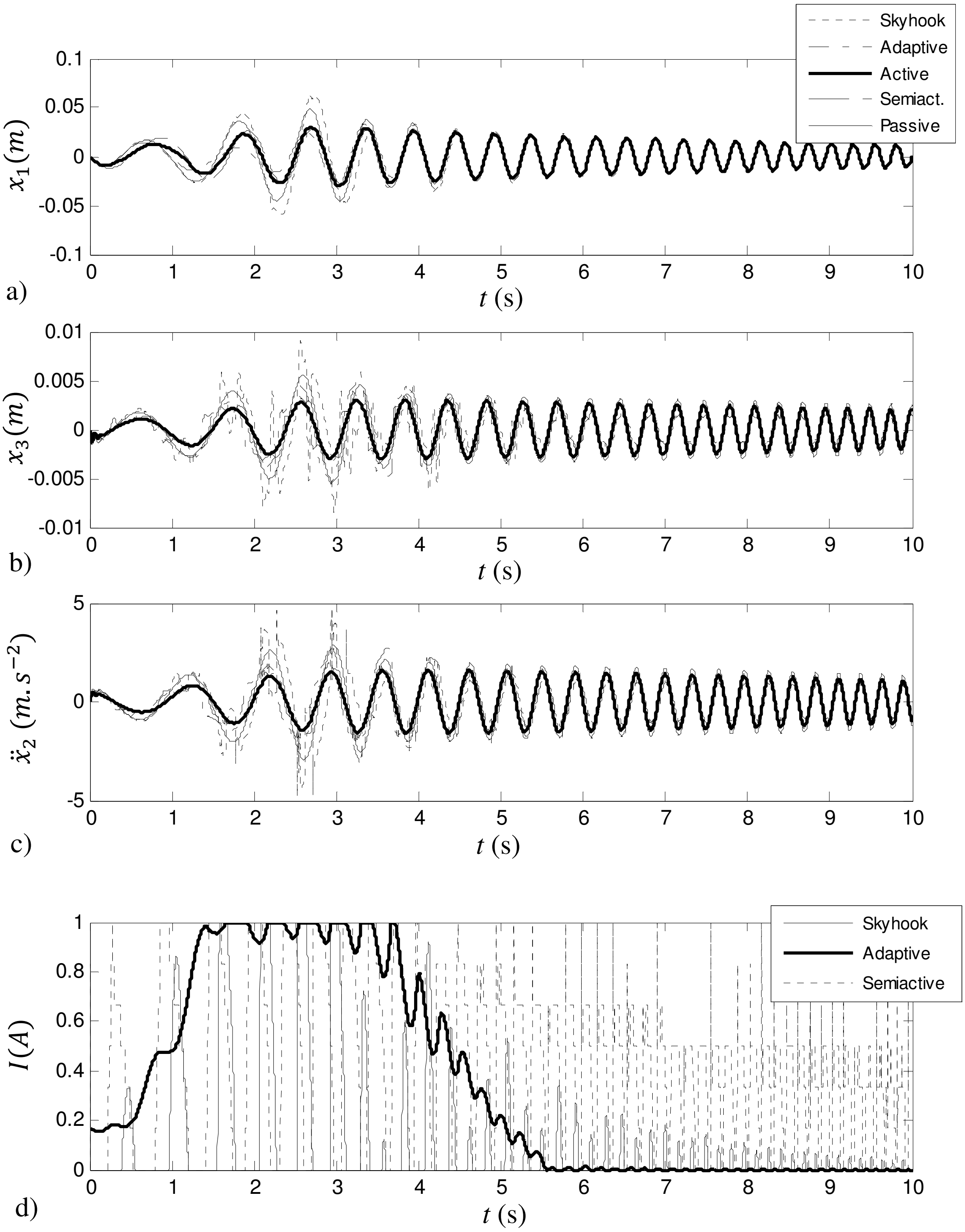

Fig. 5: The results of the sweep sine simulation

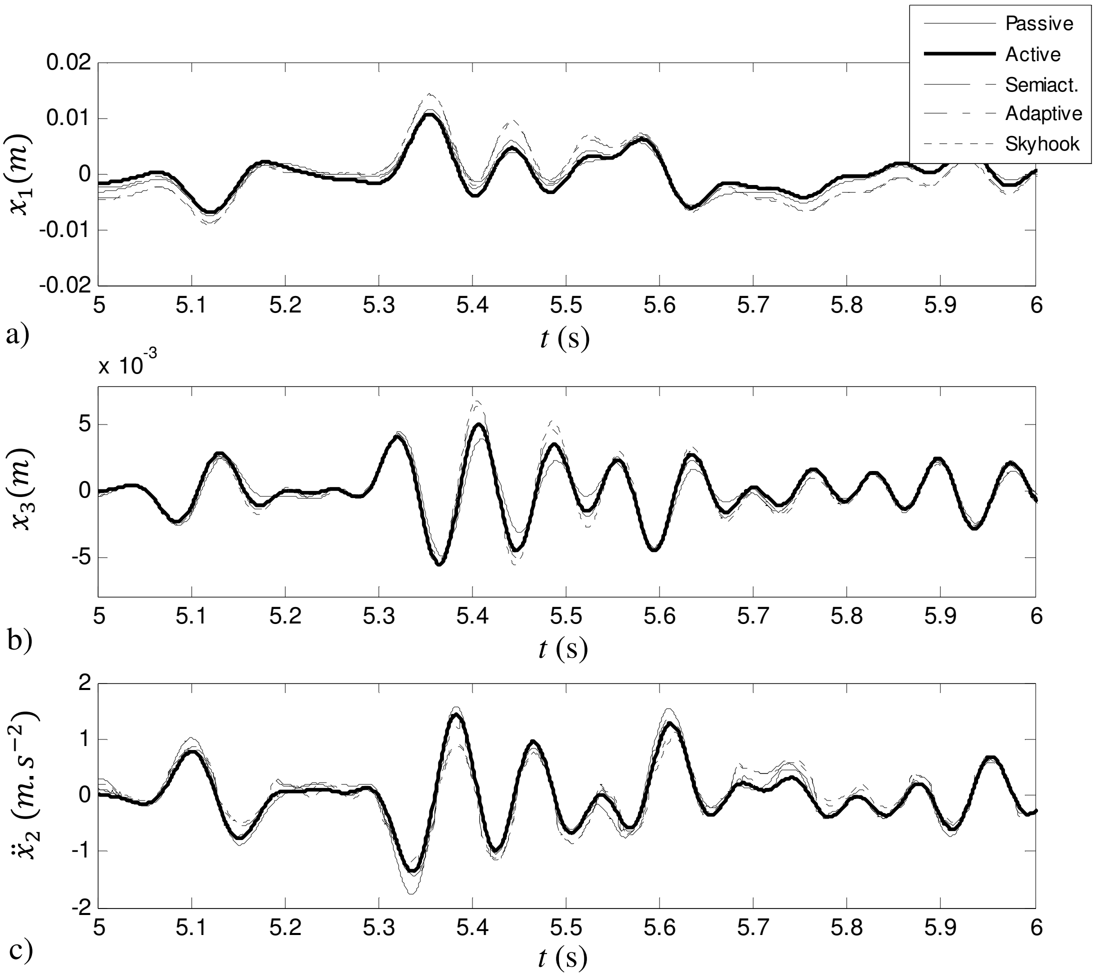

Fig. 6: The results of the random road simulation

Tab. 2: The performance index comparison among the different suspensions

	Active LQR		Semiactive LQR		Adaptive	
	J	J_{acc}	J	J_{acc}	J	J_{acc}
Sweep sine	2.0963	0.8657	2.3715	1.1251	2.6207	1.3248
Random	0.3889	0.1974	0.3942	0.2137	0.4198	0.2147

	Skyhook		Passive	
	J	J_{acc}	J	J_{acc}
Sweep sine	3.6956	1.3286	3.7586	1.7546
Random	0.4263	0.1825	0.4376	0.2751

The response of the system to the swept sine excitation over the 10 second interval is shown in Fig.5. In particular plot a) shows relative displacement of the sprung and un-sprung mass, plot b) relative displacement of the road and un-sprung mass, plot c) acceleration of the sprung mass, plot c) The current I variation for the individual control strategies over the 10s time interval.

The response of the system to the random road excitation is shown in Fig.6. The plots show the same variables as in Fig.5, but just over the 1 second time interval.

Worse performance can be seen in the case of the skyhook control near the resonant frequency. Amplitudes of the relative suspension displacement are even bigger than in the case of the passive suspension. Higher harmonics due to sudden switching of the current I can be clearly seen. Skyhook shows better performance in higher frequency excitation.

The adaptive control shows quite smooth response to the excitation signal. In contrast to the skyhook, current I varies much smoother and doesn't cause such sharp nonlinearities to the system.

The best performance clearly shows the active suspension even though the LQR theory expects the pure white noise signal accessing the system.

The semiactive LQR suspension very closely follows the active one and shows the best results among the all mentioned strategies.

In the Tab.2 are shown the simulations results in terms of the performance index. J means the overall performance index whereas J_{acc} is the part of the performance index including just the acceleration of the sprung mass, by reason of compare individual control strategies in terms of driving comfort.

According to the Tab.2 the best results shows the active suspension followed by the semiactive LQR control in booth sweep sine and random excitation. The third place takes the adaptive control followed by the skyhook and the passive suspension. If the skyhook and passive suspension is compared, it is clearly seen that the skyhook control improves riding comfort at the expense of the other two parts of the performance index. In the case of the random excitation the skyhook overcomes booth the semiactive LQR and also the adaptive control in the terms of riding comfort.

6. Conclusions

Four different types of car suspension configuration have been studied in this paper.

Hysteretic MR damper model has been formulated to predict the MR damper force and simulate suspension dynamics. This model is capable to describe nonlinear hysteretic behavior of the real MR damper. Further, MR damper model allows easy derivation of the performance index sensitivity to the control current which allows implementation of the gradient-based adaptive control algorithm.

In the simulations the best performance reached the active LQR suspension. Among the semiactive suspension, using the MR damper, the best overall performance showed the semiactive LQR control followed by the adaptive control. Even though the skyhook control reached worse performance, it is still capable to significantly improve the riding comfort over the passive suspension. In proper combination with the passive suspension elements or in the case of possible adaptation of the skyhook gain it could be efficient low cost strategy easy to implement to the real vehicle suspension.

Adaptive algorithm showed good stable performance in booth simulations. To make the general conclusion over the mentioned algorithm, stability of this nonlinear control should be closely studied, what is the subject of the next research.

References

Ahmedian, M. & Reichert, B. A. (2001) System nonlinearities induced by skyhook dampers, Shock and Vibration, Vol. 8, No. 2, pp. 95 – 104.

Crosby, M. J. & Karnop, D. C. (1973) The Active Damper. The Shock and Vibration Bulletin 43, Naval Research Laboratory, Washington, DC.

Giua, A. & Melas, M. (2004) Design of a Predictive Semiactive Suspension System. Vehicle System Dynamics, Vol. 41, No. 4, pp. 277-300.

Hong, S. R. & Choi, S. B. (2005) A hydro-mechanical model for hysteretic damping force prediction of ER damper: experimental verification. Journal of Sound and Vibration, 285, pp. 1180-1188.

Song X. & Ahmedian M. (2004) Study of Semiactive Adaptive Control Algorithms with Magneto-Rheological Seat Suspension. SAE International.

Tewari, A. (2002) Modern Control Design With Matlab and Simulink. Indian Institute of Technology, Kanpur, India.

Thomson, A. G. (1976) An Active Suspension With Optimal Linear State Feedback. Vehicle System Dynamics, 5, pp. 187-203.